

Highly Conductive Oriented PEO-Based Polymer Electrolytes

D. Golodnitsky, E. Livshits, E. Peled*

School of Chemistry, Tel Aviv University, Tel Aviv 69978, Israel
E-mail: golod@post.tau.ac.il

Summary: This contribution presents an overview of the study of the effect of stretching on semicrystalline and amorphous complexes of poly(ethylene oxide) (PEO) with different salts, such as lithium iodide, lithium trifluoromethanesulfonate, lithium hexafluoroarsenate, lithium bis(oxalato)borate and lithium trifluoromethanesulfonimide. In spite of the conventional belief that ion transport in polymer electrolytes (PE) is mediated primarily by polymer segmental motion, we suggest that ion transport occurs preferentially along the PEO helical axis, at least in the crystalline phase. It was found that the more amorphous the PE, the less its lengthwise conductivity is influenced by stretching. It is suggested that the rate-determining step of ion conduction in semicrystalline LiX:P(EO)₂₀ polymer electrolytes below the melting point (T_m) is "interchain" hopping.

Keywords: "interchain" hopping; ion transport mechanism; orientation; PEO; polymer electrolyte

Introduction

The possibility of using polymer electrolytes (PE), as the basis of high energy-density batteries was first recognized by Armand^[1] about two decades ago and is a driving force behind the research performed on these materials. The polymer electrolyte plays three important roles in the battery: 1. The polymer electrolyte is a ion carrier and can be formed into large-area thin films, which lower internal cell resistance even for electrolytes with moderate conductivity; 2. The polymer electrolyte functions as an electron separator electrochemically compatible with highly reactive anodes and cathodes; 3. The polymer electrolyte is a binder of cathode active material. In addition to the variety of technological applications, solvent-free polymer electrolytes are of interest as model materials for the investigation of conduction paths in semicrystalline (partially ordered) systems.

The driving force for the dissolution of a salt in both liquid and solid media is described by the well known thermodynamic relationship:

$$\Delta G = \Delta H_m - T\Delta S_m$$

The mixing enthalpy, ΔH_m , includes the lattice energy of the salt, the lattice energy of the solvent, the Coulombic ion-ion interaction energy, and the ion solvation energy.^[2-5] In most investigations, the mixing enthalpy is assumed to be the dominant factor in the solubility of the salt in the polymer. The mixing entropy consists mainly of two components: translational and configurational. Contrary to the case of water, the mixing entropy for the formation of polymer electrolytes is small or even positive. The incorporation of salts into the polymer inevitably reduces the freedom of polymer chain motion, thus causing the reduction in translational entropy. The configurational entropy of mixing depends mainly on the available coordination sites in the polymer, which are affected by spacing between sequential coordination sites and by steric effects. Ion transport in polymer electrolytes is a complex process that includes long-range ion motion, local motion of polymer segments and inter- and intrapolymer transport between ion-coordinating sites. In this case, the conduction sites are not fixed; instead, the solvent site positions appropriate for cation bonding vary with time. The segmental movement of the polymer chain creates new sites and removes old one. Therefore, the conductivity, which is generally observed to rise with increasing the amorphousness of the polymer electrolyte, is closely connected with increased flexibility of the chains and rapid relaxation of the host polymer.

Semi-crystalline solid (PEO), which is the most intensively studied host polymer for polymer electrolytes has an extended helical structure with repeat units, consisting of seven $-\text{O}-\text{CH}_2-\text{CH}_2-$ groups in two turns of the helix. Bruce and coworkers^[6,7] were the first to show that in the polymer-salt complex, PEO chains are wrapped around the cation with each Li^+ coordinated by three ether oxygens from the polymer chain. The intra-helix location of the cations, and possible ion motion along the helix suggested by Armand^[1] give reason to expect that alignment of the polymer chains should be followed by an increase in ionic conductivity.

With this in mind we have recently tested semicrystalline complexes of poly(ethylene oxide) (PEO) with LiI under expanding load. Stretching induced DC conductivity enhancement by a factor of 5-40 was observed in $\text{LiI}:\text{P}(\text{EO})_n$ films in spite of the formation of more ordered PE structure and reduced segmental motion.^[8-11] In the current contribution we give an overview of our study of the complex interplay between ionic transport processes and macroscopic order in semicrystalline and amorphous PEO-based polymer electrolytes with different salts, such as

lithium iodide, lithium trifluoromethanesulfonate, lithium hexafluoroarsenate, lithium bis(oxalato)borate and lithium trifluoromethanesulfonimide.

Experimental

The electrolytes were prepared from poly(ethylene oxide) (PEO) (Aldrich, average molar mass 5×10^6), which was vacuum dried at 45 to 50 °C for about 24 h. The lithium salts (Aldrich) were vacuum dried at 150 °C for about 24 h. Lithium bis(oxalato)borate was synthesized by Wu Xu.^[12] All subsequent handling of these materials took place under an argon atmosphere in a VAC glove box with water content <10 ppm. The thickness of the solvent-free films was 150 μm . The films were cut, hot pressed together with the incorporated four 0.05mm-thick wire electrodes as shown in.^[8-11] Experimental details of the preparation and stretching of PEs is described elsewhere.^[9-11,13] Longitudinal conductivity measurements during stretching were performed in the galvanostatic mode with the use of four electrodes. Four-probe-DC *in-situ* measurements were carried out in accepted manner; namely, the voltage drop across the known resistance of 8-100 M Ω was measured and the calculated current was used to extract the unknown polymer electrolyte resistance from a measurement of the voltage drop between two internal electrodes. The voltage measurements were taken every 15 s under lengthwise extending load.

The AC conductivity in the perpendicular direction was measured *ex-situ* with the use of a Solartron 1255 frequency-response analyzer controlled by a 586 PC over the frequency range 1MHz-0.1Hz. The polymer electrolyte sample of 1cm² area was placed between two lithium electrodes under a spring pressure of 5 kg/cm². The configuration of the cell is described in.^[14] The accuracy of the calculation of bulk resistance (R_b) is estimated to be about $\pm 10\%$.

The samples for DSC measurements were prepared in a VAC glove box. They were hermetically sealed in alodined (covered by high resistant and compact surface oxide film) aluminum DSC pans. The DSC tests were carried out with TA Instruments module 2010 and System Controller 2100 at a scan rate of 10 deg/min up to 150 °C.

A JSM-6300 scanning microscope (Jeol Co.) equipped with a Link elemental analyzer and a silicon detector was used for the study of surface topology.

X-ray diffraction data were obtained with the use of a Θ - Θ Scintag powder diffractometer equipped with Cu K α source and liquid nitrogen germanium solid-state detector. Films were

mounted on background free single crystal quartz slides and isolated from the atmosphere by 7 μm thick aluminum film.

Results and Discussion

We began this study of the effect of stretching on ion transport with $\text{LiI}:\text{P}(\text{EO})_n$ solid polymer electrolytes. Up to an extension load from of 400 N/cm^2 along the polymer specimen, neither polymer electrolyte resistance nor visible sample changes were observed. Under the load of $450\text{--}800 \text{ N/cm}^2$ the samples began to flow and the DC conductivity increased by a factor of two to forty, depending on the $\text{EO}:\text{Li}$ ratio and stretching conditions. After removal of the load stretched polymer electrolytes retained high ionic conductivity in the axial direction for at least two weeks. In [11, 13] it was shown that temperature increase from room temperature to about the melting point of the PEO (65°C) is followed by almost a five-fold increase in the conductivity of dilute $\text{LiI}:\text{P}(\text{EO})_n$ electrolytes (with $20 \leq n \leq 100$). The stretching process was found to influence the DC conductivity in the direction of the applied force more strongly than does an increase in temperature. The maximal conductivity enhancement (about 40 times) in the direction of applied force was found in the $\text{LiI}:\text{P}(\text{EO})_7$ electrolyte with highly elastic structure. As soon as the tension on the sample is released, the film shows elastic behavior, undergoing considerable shrinkage. Nevertheless, The absolute longitudinal conductivity of the stretched $\text{LiI}:\text{P}(\text{EO})_7$ electrolyte approaches 0.1 mS/cm at 25°C .

In order to determine whether this phenomenon is unique to LiI -PEO electrolytes or is the rule for PEO-based systems, we tested PEs with different salts.^[15] The experimental data of in-situ longitudinal DC-conductivity ($_{\parallel}\sigma_{\text{DC}}$) measurements of the polymer electrolytes at room temperature are shown in Fig. 1.

The stretching process was found to increase the $_{\parallel}\sigma_{\text{DC}}$ of the $\text{LiI}:\text{P}(\text{EO})_{20}$, and $\text{LiTF}:\text{P}(\text{EO})_{20}$ PEs more strongly (by about a factor of 10 to 16) than that of $\text{LiBOB}:\text{P}(\text{EO})_{20}$ and $\text{LiTFSI}:\text{P}(\text{EO})_{16}$ PE (factor of 6). It is noteworthy that the absolute $_{\parallel}\sigma_{\text{DC}}$ value of the $\text{LiTFSI}:\text{P}(\text{EO})_{16}$ PE is $2.5 \cdot 10^{-6} \text{ S/cm}$ at room temperature, three times that of the other PEs under investigation. After stretching, the longitudinal conductivity of all the polymer electrolytes is the same order of magnitude ($0.8\text{--}1.5 \cdot 10^{-5} \text{ S/cm}$). Note that stretching-induced conductivity enhancement by a factor of only three was measured in $\text{LiTF}:\text{P}(\text{EO})_7$ electrolyte, unlike $\text{LiI}:\text{P}(\text{EO})_7$ where the longitudinal conductivity increased from $2.5 \cdot 10^{-5} \text{ mS/cm}$ to

0.1mS/cm, as a result of stretching. As expected, the longitudinal conductivity enhancement was found to be inversely proportional to the rate of stretching. While the elongation of the LiTF:P(EO)₂₀ film was almost the same (430-490%) at rates of 10 and 50mm/min, the conductivity increased by a factor of 16 and 5, respectively. This is because the time for the re-orientation of polymer chains is insufficient.

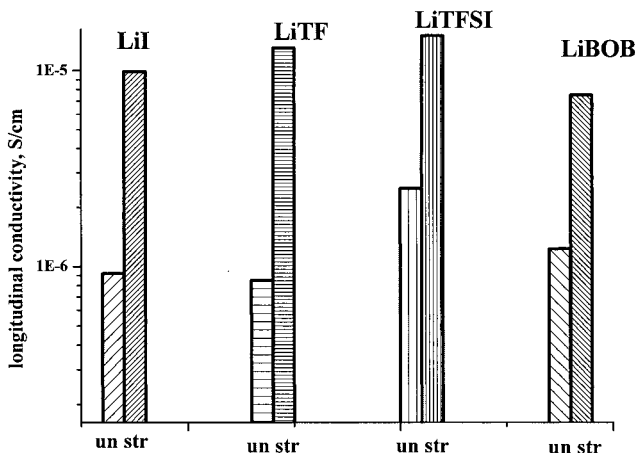


Fig. 1. In-situ longitudinal DC conductivity data of LiX:P(EO)_n polymer electrolytes.

Conductivity measurements in the direction perpendicular to the applied force were performed *ex-situ* in a Li/PE/Li cell. It is well established that ionic conduction in PE systems is governed by a complex interplay of two mechanisms. One is associated with ion transport along directed molecular structures like the helical chains in PEO; the other, strongly dependent on the host segmental motions, is controlled by ion hopping between such structures. Impedance spectroscopy is a good experimental tool for studying ion-transport processes in solid polycrystalline electrolytes. Typical complex impedance (Nyquist) plots for unstretched polymer electrolyte, shown in Fig. 2, is represented by two partially depressed semicircles.

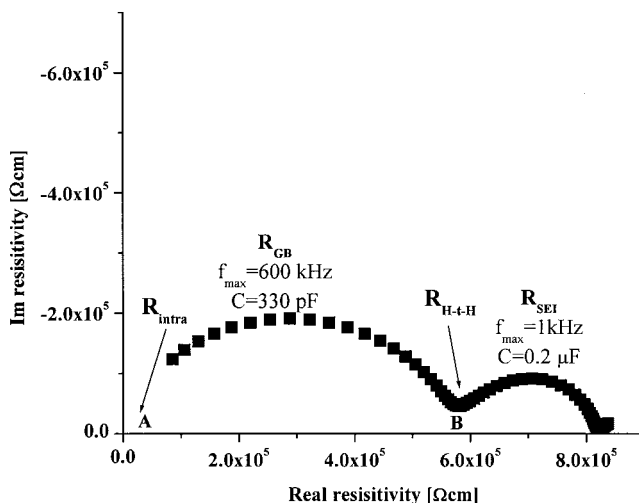


Fig. 2. Nyquist plot of unstretched LiTFSI:P(EO)₁₆ polymer electrolyte measured in the direction normal to stretching.

The arc with f_{\max} 1 kHz is associated with the resistance of the passivating film (solid electrolyte interphase (SEI)) generated on the lithium electrode in contact with the electrolyte.^[16] The introduction of a second time constant in the equivalent circuit (high-frequency arc with f_{\max} in the range 0.05 to 1 MHz, and capacitance from 50 to 200 pF/cm²) may be attributed to the grain-boundary resistance (R_{GB}), which includes contributions of hindered helix-to-helix jump (R_{H-H}). The GB semicircle disappears from the Nyquist plot of the unstretched LiTF PE at about 65°C, and at about 35-40°C from the plot of LiTFSI PE. The ionic conductivity of polymer electrolytes associated with intrachain (or intrahelix) ion mobility is calculated from the high-frequency intercept of this arc with axis X (marked as R_{intra}). It was found that the intrachain ionic conductivity of polymer electrolytes in the direction normal to the applied tensile force, decreases as a result of stretching. The absolute values of the $\perp\sigma_{intra}$ of the unstretched sample are 6 to 10 times higher than that of the stretched sample at room temperature for the LiTF electrolyte. At above 65°C this difference vanishes. For LiTFSI PE $\perp\sigma_{intra}$ of the stretched film is lower by a factor of three at RT and at about melting point of the eutectic it approaches that of the unstretched film. Lower $\perp\sigma_{intra}$ values of the stretched PEs can

be explained by alignment of the PEO helices in the direction of the force, and, as a result, very few helices oriented in the orthogonal direction are left.

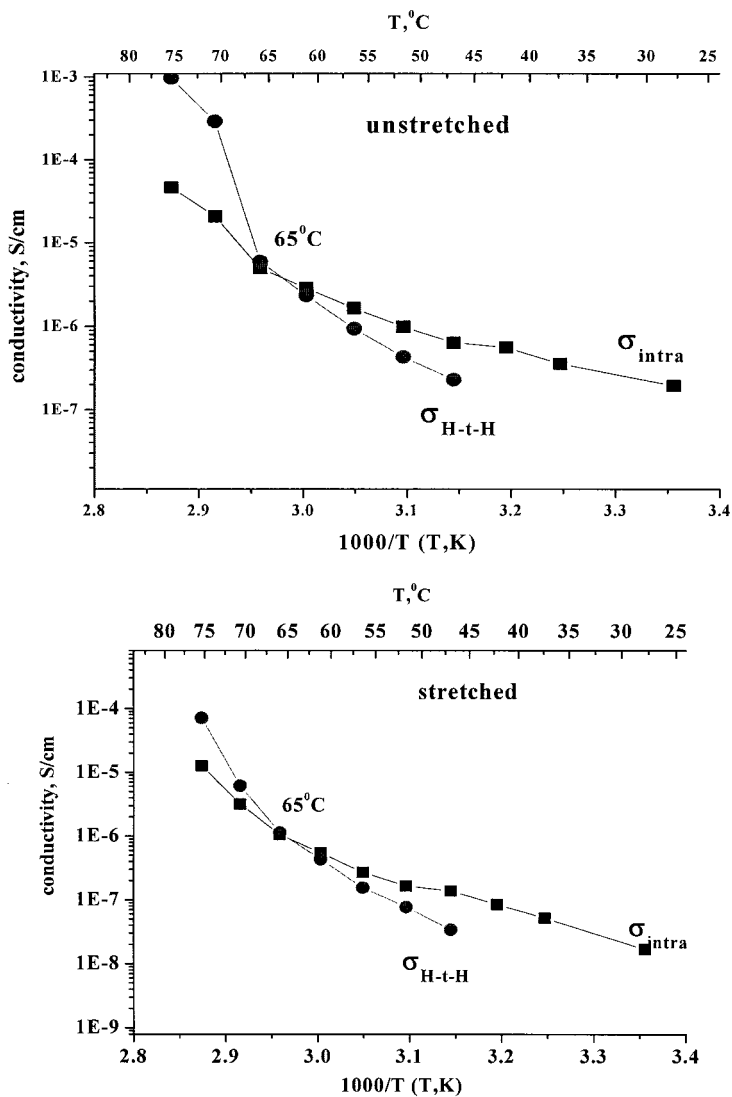


Fig. 3. Arrhenius plots of inter- and intrachain conductivity in the normal to applied tensile force direction of the unstretched and stretched LiTF:P(EO)₂₀ polymer electrolyte.

The conductivity related to ion-hopping between different molecular chains or segments of the PEO in the normal direction ($\perp\sigma_{\text{HtH}}$), calculated from the low-frequency intercept of the GB arc with axis X (marked as R_{HtH}) is lower by about a factor of five for the stretched PEs as well. The difference in $\perp\sigma_{\text{HtH}}$ between unstretched and stretched PEs is almost unaffected by temperature up to 65°C for LiTF, LiAsF₆ and LiI electrolytes. Fig. 3 shows Arrhenius plots of both $\perp\sigma_{\text{intra}}$ and $\perp\sigma_{\text{HtH}}$ of unstretched and stretched LiTF-PEs. A comparison of intra-chain with inter-chain ion mobility shows that bulk intra-helix conductivity in the LiTF-P(EO)₂₀ electrolyte at room temperature is about one order of magnitude higher than that of the helix-to-helix jump. At above 65°C the converse is true. We believe that this is good evidence of preferential lithium-ion transport along the PEO helical axis, at least in the crystalline phase. It is suggested that for LiI and for LiTF as well below T_m the rate-determining step of the lithium ion conduction process is the inter-chain hopping. Above 65°C the rate-determining step changes. For unstretched LiTFSI and LiBOB-PEs, however, even at room temperature helix-to-helix hopping is faster than intra-chain ion mobility. For the stretched samples of these PEs the bulk and hopping conductivity values are close. Another interesting observation is that in as-cast LiI and LiTF PEs the longitudinal DC conductivity is two to three orders of magnitude higher than the sum of orthogonal $\perp\sigma_{\text{intra}}$ and $\perp\sigma_{\text{HtH}}$ values (Fig. 4). This indicates that cast semicrystalline PEs present high degrees of uniplanar orientation, corresponding to the tendency of the crystallographic planes of the helix to be parallel to the film plane. On stretching, the difference increases by up to four orders of magnitude. In the unstretched LiBOB and LiTFSI solid polymer electrolytes the lengthwise and normal conductivity values are similar.

It will be noted that the longitudinal DC conductivity rise is directly proportional to the yield strength. This may indicate that the reorientation ability is closely linked to the amount of crystalline phase in the PE. Polymer-salt complexes of polyethylene oxide (PEO) have a high degree of crystallinity and these crystalline phases represent well-defined stoichiometric structures.^[17,18] Depending on the composition and temperature, these systems also contain either the pure crystalline polymer or an amorphous phase. DSC examination of the unstretched PEs under investigation (Fig. 5-dashed curves) clearly shows the shift toward low temperature of the glass transition point (T_g) from 13 to -34°C and onset of the melting endotherm from 60 to 35°C in LiTF-based and LiImide-PEO PEs, respectively. The height of the peak decreases by a

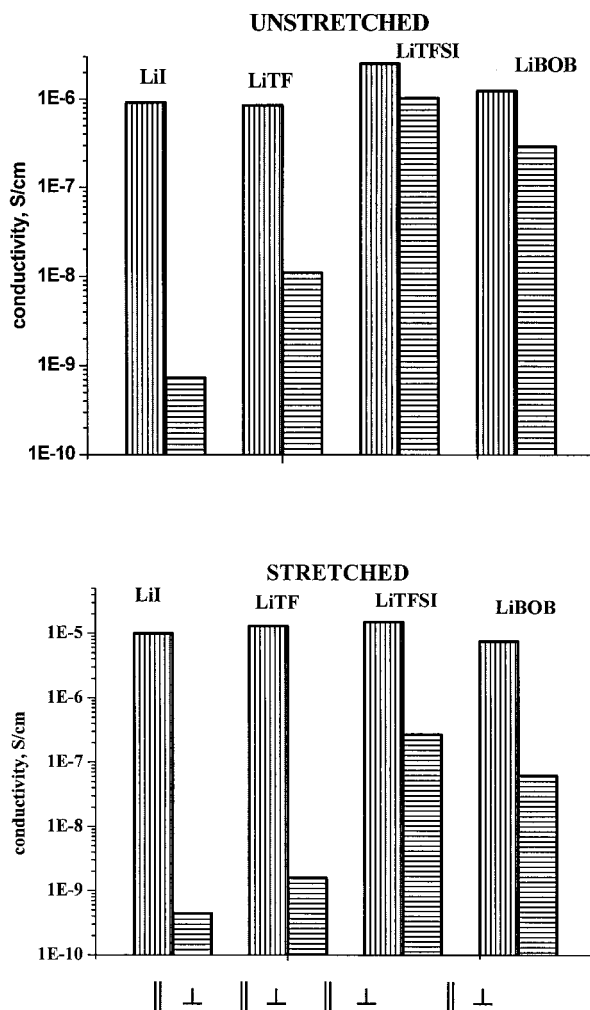
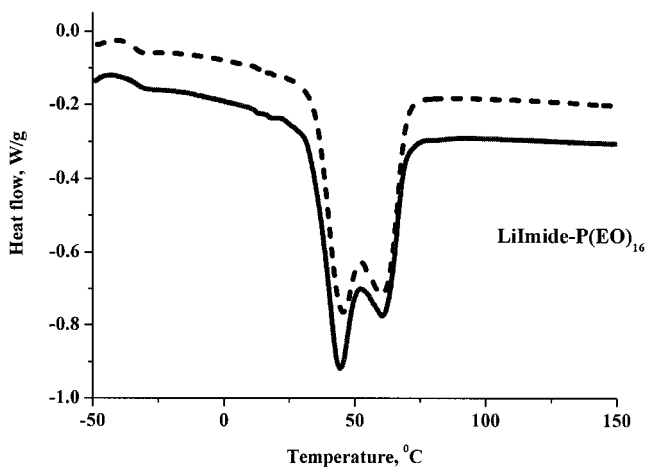


Fig. 4. Longitudinal and normal conductivity.

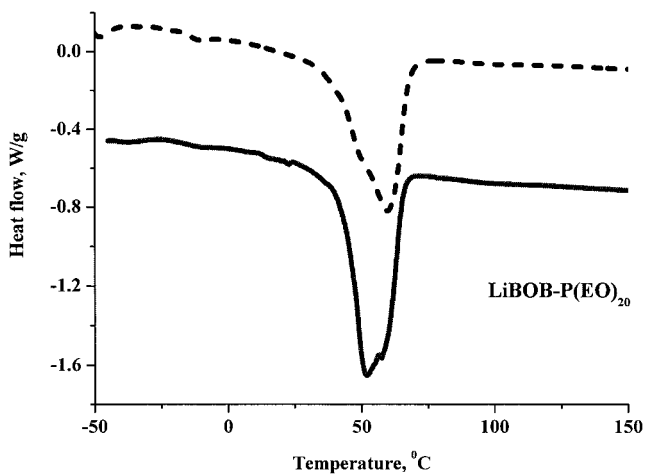
factor of two and its width increases. This is in agreement with published data, where LiTF is shown to form crystalline 3:1, 4:1, and 6:1 complexes with PEO, and LiTFSI-PEO complexes

are amorphous. It is well known that PEO electrolytes containing lithium trifluoromethanesulfonimide have high ionic conductivities; this is due both to the low lattice energy of this lithium salt, which facilitates the solvation of lithium by the polyether, and to the large anion, which hinders the crystallization of the PEO and salt mixtures.^[18] It should be mentioned, however, that the enthalpy of melting is little affected by the type of salt and varies in the range of 90 to 115 J/g. The different shapes of the melting peaks, the strong dependence of their height and width on the type of salt, but similar enthalpy values indicate that the degree of crystallinity in the polymer electrolytes may be related to the different extent of orientation of the uncomplexed PEO chains. Fig. 5 shows the DSC traces of both unstretched (dashed curve) and stretched (solid curve) polymer electrolytes. When the films are stretched, the dependence of T_g and T_{on} on the type of salt remains. The peaks, except those for LiTFSI-PE, become significantly narrower as a result of stretching. This is followed by a 20% increase in their height for, suggesting that alignment of polymer chains makes the polymer electrolyte more ordered. The enthalpy of the low-temperature melting transition of both the stretched LiBOB and LiTFSI electrolytes, which can be assigned to the melting of a eutectic, dramatically increases on stretching, at the expense of the liquidus peak.

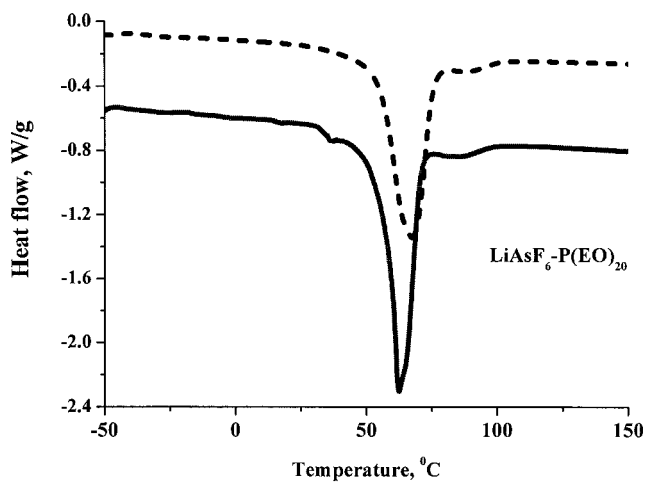
a)



b)



c)



d)

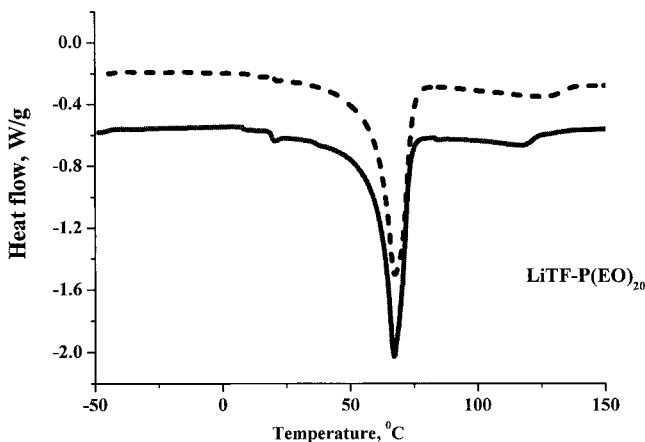


Fig. 5. DSC thermograms of unstretched and stretched polymer electrolytes.

All the polymer electrolytes under investigation exhibit clear grain crystalline structure. Fig. 6 shows SEM micrographs of unstretched LiX-P(EO)_n films where $n=16$ for LiTFSI , and $n=20$ for other PEs. The surface of LiX:P(EO)_{20} , as well as net PEO, presents a multitude of compacted grains of 50 to 100 μm size. At high magnification ($\times 5000$) the topography of most films is very homogeneous and individual grains could not be resolved. Likewise, the LiI PE stretching of other polymer electrolytes under investigation is followed by the formation of unidirectionally oriented fiber-like microphases of several micron width as shown in Fig. 6. The stretched LiTFSI-P(EO)_{16} undergoes non-uniform plastic deformation. Two different regions, namely: aligned oriented fibers and the remains of crystallites can be distinguished in the SEM images of this sample. We would like to emphasize that LiI-P(EO)_7 , unlike the other PEs, was found to have a highly elastic structure, the stretching of which was followed by the formation of aligned oriented regions of several tenths of a micron width.^[11] Bruce and co-workers found for LiAsF_6 that the 6:1 EO:Li complex forms double non-helical chains which interlock to form a cylinder.^[19, 20] The lithium ions reside inside these cylinders and, in contrast to other complexes, are not coordinated by the anions. Such double-helix structure should facilitate fast ion migration and is in agreement with the high values of stretching-induced longitudinal conductivity of LiI-P(EO)_7 (0.1 mS/cm), presented above.

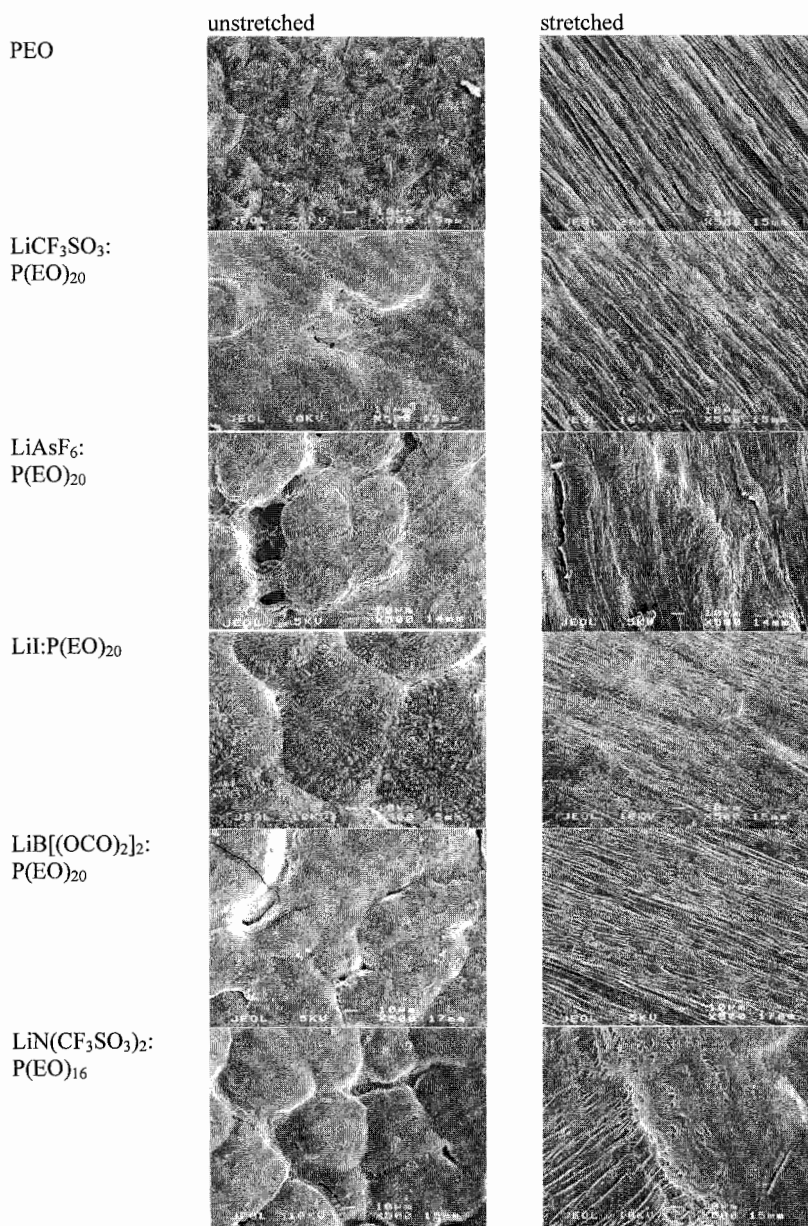
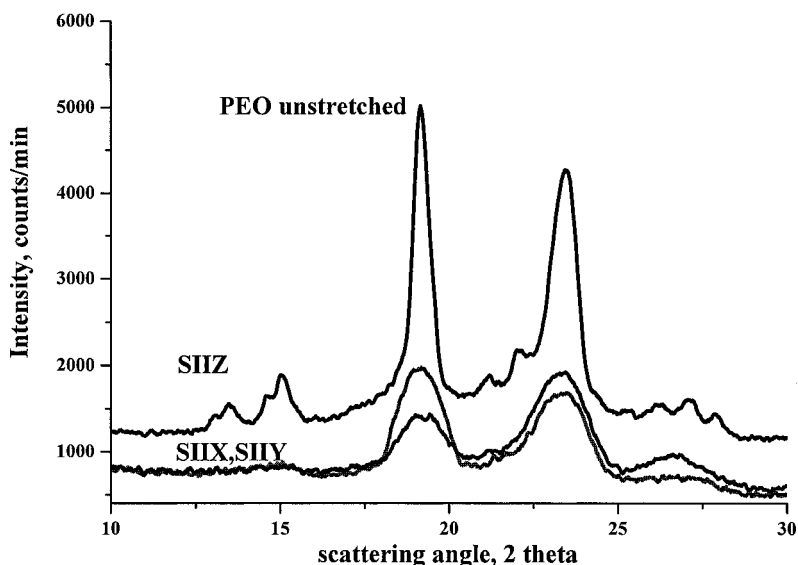


Fig. 6. SEM micrographs of the polymer electrolyte films.

We have suggested^[13] that there are at least three degrees of stretching-induced structural long- and short-range order. This suggestion stems from the analysis of AFM images, XRD, IR and NMR spectra. Structural ordering imposed by stretching was observed in AFM images of pure PEO, LiI:P(EO)_n ^[13] LiTF and LiTFSI:P(EO)_n electrolytes. The as-cast polymer- electrolyte films are built from several micron-size randomly oriented separate domains. Each domain, in turn, is composed of either partially aligned or entangled fibers. The individual fibers, however, can not be resolved in the AFM images of LiTFSI:P(EO)_n PE even at high magnification. Upon stretching, the large separate units as well as the fibers gain a preferred orientation. The average diameter of the individual fibers is about 40-50 Å. It seems likely that each fiber, in turn, contains several helical PEO macromolecules.

Fig. 7a shows comparative XRD data of the unstretched PEO film in reflection and transmission modes. The upper curve was obtained in reflection mode with the scattering vector parallel to Z axis. Diffraction patterns obtained in the transmission mode with the scattering vector parallel to X and Y axes are almost completely identical. By analogy with XRD of polyethylene^[21] and according to the XRD data presented in,^[6,11] we suggest that the observed Bragg peaks are associated with the PEO helical axes lying in the corresponding scattering planes. From the XRD patterns, therefore, it is deduced that in unstretched samples, oriented crystalline helical microphases are uniformly distributed across the thickness of the sample with preferable longitudinal orientation of some aligned microphases. Fig. 7b presents the XRD patterns of the stretched samples. On stretching, the relative intensity of the peaks appearing at 19.4 and 23.5 deg. changes and the XRD pattern from the YZ plane (scattering vector parallel to the X-axis) PE is represented by a single Bragg peak, indicating a more uniformly oriented PE structure. The bottom curve corresponds to the diffraction pattern of the stretched sample in transmission mode with the scattering vector parallel to Y axis. The disappearance of Bragg diffraction lines in this geometry demonstrates that the stretched sample does not contain oriented helical microphases lying in the XZ plane (that is, they are now preferentially oriented perpendicular to the XZ plane; i.e. along Y). From the plots presented in the Fig. 7a and b it is obvious that the XRD patterns of net PEO are identical to those of the polymer electrolytes. While there is a subtle indication of the halo in the XRD patterns of the LiTFSI electrolyte, which is known to form amorphous complexes with PEO, the main tendency of the stretching induced re-orientation is retained in this electrolyte too. We believe that each Bragg peak can

be associated with a separate assembly of crystalline microphases of oriented PEO helices. The broad component (peak at 23.5 deg.) corresponds to only slightly oriented segments of the helix with interplanar space $d = 3.7\text{\AA}$. The narrow component (peak at 19.5 deg) with $d = 4.6\text{\AA}$ may be assigned to the microphases of almost perfectly oriented extended helical chains, composed of stretched macromolecules. On stretching of the PE the intensity of this Bragg line increases dramatically, indicating an increase in the content of extended macromolecules at the expense of microphases of slightly oriented helices. XRD data unambiguously show that the stretching process of the PEO-based electrolytes with different salts converts a film with a random distribution of helical crystalline microphases into a textured one. As expected, the preferred texture orientation coincides with the stretching direction. It seems likely that these are the Bragg lines of uncomplexed crystalline PEO, which are mainly affected by stretching.



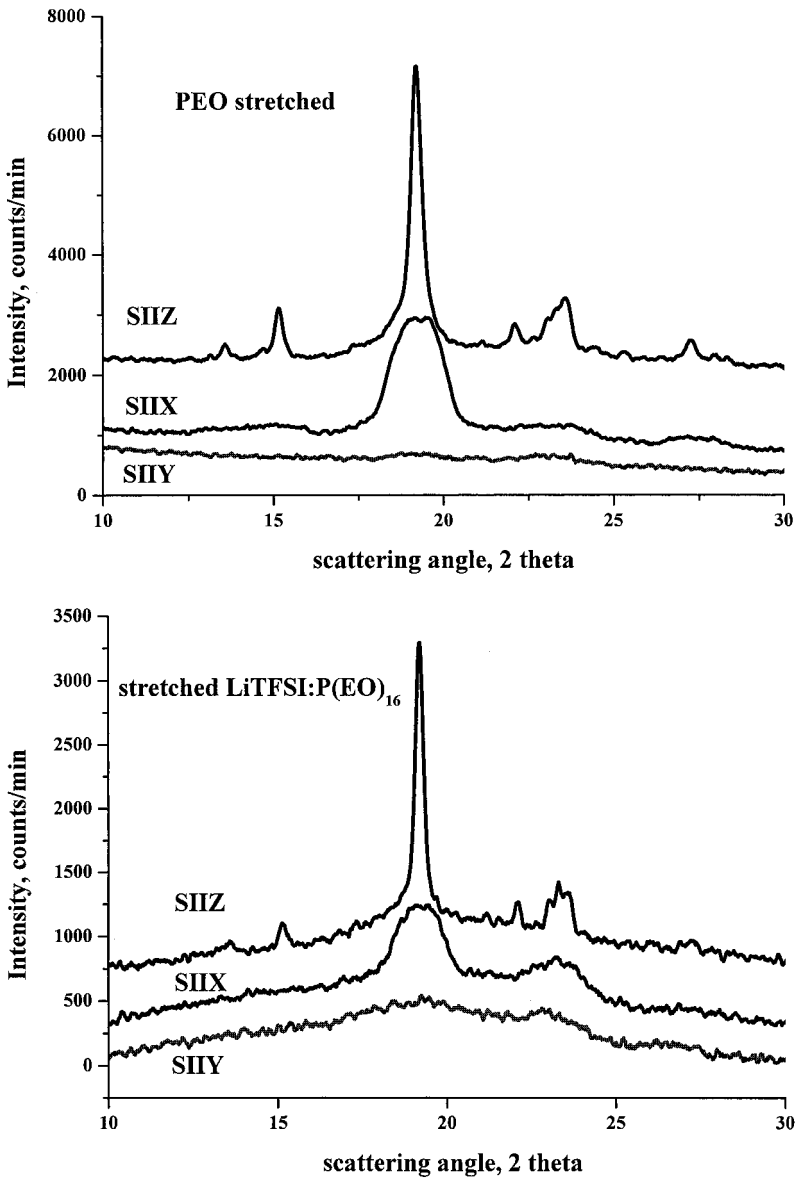


Fig. 7. XRD patterns of PEO and LiTFSI:P(EO)₁₆ films.

FTIR measurements carried out on the LiI-P(EO)_n polymer electrolytes^[13] showed that the IR spectra of stretched dilute LiI:P(EO) PEs responsible for skeletal CCO and COC bending, stretching and CH_2 rocking vibrations, are similar to those of the stretched PEO. This shows that application of tensile force to the film affects mainly the polymer phase and not the complex. This is in agreement with the XRD data. In the concentrated PEs, the effect of stretching on the skeletal stretching vibrations of the C-O and C-C bonds and CH_2 rocking mode is less pronounced. We suggest that in concentrated polymer electrolytes, formation of ion aggregates (like $\text{Li}^+\text{-I}^-\text{Li}^+$) bridges the ether oxygens of adjacent chains, thus preventing the strong effect of stretching. The broadening of the bands and their frequency shift toward low energies, observed as a result of stretching of even concentrated polymer electrolytes, may indicate that the stretching process favors such conformational changes of coordinative groups in the polymer chain that level the effect of salt addition to the PEO. This may result in the regaining of the original extended open-helix shape typical of PEO itself. In agreement with^[22-24] we suggest that conformational changes in the PEO-LiI complexes are achieved by a change in the torsional O-C-C-O angle, which has a very low rotational-energy barrier. In the aligned helical structure of the stretched polymer electrolyte, the CH_2 groups all face outwards and the atoms of oxygen are directed inward. The lining of the tunnel cavity and the creation of the energetically beneficial conduction paths should follow the stretching process. The stretching- induced longitudinal conductivity enhancement supports our suggestion.

The diffusion coefficient along the stretched direction in LiI:P(EO)_9 PE detected by pulse NMR was almost four times that in the orthogonal direction.^[13] This data supports the notion that Li^+ diffusivity is enhanced by alignment of the helical structural units of the polymer and that segmental motion mediated by ion-hopping is not the only conduction mechanism. In LiI PEs, because of the lack of suitable NMR nuclei in the anion, the relative role of the cations and anions in the enhanced conductivity could not be ascertained. The NMR tests of stretched LiTF and LiTFSI electrolytes are in progress and will be published soon.

Conclusions

Poly(ethylene oxide)-based solid polymer electrolytes with different salts, such as lithium iodide, lithium trifluoromethanesulfonate, lithium hexafluoroarsenate, lithium bis(oxalato)borate and lithium trifluoromethanesulfonimide were characterized by DSC, SEM,

XRD and electrochemical methods. It was found that molecular architecture plays an important role in determining the ionic conductivity of polymer electrolytes and that ion transfer is driven by competing inter- and intramolecular ion-polymer chain interactions. Stretching-induced longitudinal-DC-conductivity (σ_{DC}) enhancement, observed in crystalline LiI-P(EO)_n and LiTF-P(EO)₂₀ electrolytes, was about 5 to 40-fold, while the increase in σ_{DC} in mostly amorphous non-uniformly stretched LiTFSI-P(EO)₁₆ PE was only 6-fold. This indicates that aligned crystalline PEO chains are energetically more favorable for fast ion transport, than are entangled chains. For high-energy-density thin-film all-solid-state batteries, however, the high ion mobility in the orthogonal direction is not less important than that in the longitudinal direction. This indicates a need for synthesis of new rigid polymers with two-dimensional ordered highly-conductive channels.

Acknowledgements

This work was supported by Israel Academy of Science (contract No 323/00-2). We thank to Dr. Wu Xu for the lithium bis(oxalato)borate sample and Dr. Yu Rosenberg from Wolfson Applied Materials Research Center of Tel Aviv University for the XRD tests.

- [1] M. B. Armand, *Ann. Rev. Matter Sci.*, **1986** 16, 245-261.
- [2] S.D. Druger, M. A. Ratner and A. Nitzan, *Solid State Ionics*, **1983** 9/10, 1115-1120.
- [3] Polymer Electrolyte Review **II**, J. R. MacCallum and C.A. Vincent Eds., Elsevier Applied Science, London and New York 1989
- [4] F. M. Gray, *Solid Polymer Electrolytes*, VCA, New York 1991.
- [5] A.Bakker, *Ionic Mobility and Molecular Vibrations in Aqueous and Polymer Electrolytes*, Ph.D thesis, Acta Univ. Ups, 1995
- [6] D. F. Shriver, P.G. Bruce. *Polymer Electrolytes I: General Principles*, *Solid State Electrochemistry*, P.G. Bruce (Ed.) Cambridge University Press, Great Britain, 1995, 95-119
- [7] Y.G. Andreev, P.G. Bruce *Electrochimica Acta*, **2000** 45, 1417-1423
- [8] D. Golodnitsky and E. Peled, *Electrochimica Acta*, **2000** 45, 8-9, 1431-1436
- [9] S. H. Chung, Y. Wang, S. G. Greenbaum, D. Golodnitsky and E. Peled, *Electrochemical and Solid-State Letters*, **1999**, 2, 11, 553-555.
- [10] D. Golodnitsky, E. Peled, E. Livshits, Yu. Rozenberg, S.H. Chung, Y. Wang, and S. Greenbaum. *Journal of Electroanalytical Chemistry*, **2000**, 491, 203-210.
- [11] D. Golodnitsky, E. Livshits, I. Lapides, Yu. Rosenberg, E. Peled, *SSI*, **2002** 147, 265-273
- [12] Wu Xu and C.A. Angell, *Electrochemical and Solid State Letters*, 4 (1), E1-E4 (2001)
- [13] D. Golodnitsky, E. Peled, E. Livshits, A. Ulus, Z. Barkay, I. Lapides, S.G. Greenbaum, S.H. Chung, Y.Wang, *Journal of Physical Chemistry, part A*, **2001** 105, 44, 10098-10106.
- [14] D. Golodnitsky, G.Ardel, E.Strauss , E.Peled, Y. Lareah and Yu. Rosenberg, *J. Electrochem.Soc.*, **1997**, 144, 10, 3484 – 3491.
- [15] D. Golodnitsky, E. Livshits, A. Ulus, E. Peled, *Polymers for Advanced Technologies*, 2002, in press
- [16] E. Peled, D. Golodnitsky, J. Pencienier Anode/electrolyte interface, in *Handbook of Battery Materials*, (Ed.,: J.O.Besenhard) Verlag Chemie (VCH), **1999**, 410-457.
- [17] F.Gray, M. Armand, *Polymer Electrolytes in Handbook of Battery Materials*, Ed.: J. O. Besenhard, Wiley-VCH, **1999** 499-520.
- [18] C.D. Robitaille and D. Fauteax, *J. Electrochem Soc.* **1986** 133, 315.
- [19] MacGlashan GS, Andreev YG, Bruce PG, *Nature*, 398, **1999**, pp.792-3.
- [20] Z. Gadgourova, Y. Andreev, D. Tunstall, P. Bruce, *Nature*, 412, **2001** 520
- [21] M. Kakudo, N. Kasai. X-ray diffraction by polymers, Kodansha Ltd. and Elseiver **1972**.
- [22] H. Matsuuda, K. Fukuhara, *Journal of Polymer Science: Part B: Polymer Physics*, **1986**, 24, 1383-1400
- [23] B. L. Papke, M.A. Ratner, D. F. Shriver, *J. Phys. Chem. Solids*, **1981** 42, 493-500
- [24] R. Frech, W. Huang, *Macromolecules*, **1995** 28, 1246-1251

